Supplement of Hydrol. Earth Syst. Sci., 23, 851–870, 2019
https://doi.org/10.5194/hess-23-851-2019-supplement

Hydrology and Earth System Sciences
Open Access
EGU

Supplement of

Linear Optimal Runoff Aggregate (LORA): a global gridded synthesis runoff product

Sanaa Hobeichi et al.

Correspondence to: Sanaa Hobeichi (s.hobeichi@student.unsw.edu.au)

Table S1: Example of weights (w) and bias ratios (r) computed for the participating products over a range of river basins.

	HBVS		HTESS1		HTESS2		JULES1		JULES2		LISF		PCRG		SURF2		SURF1		WGAP3		W3RA	
	w	r	w	r	w	r	w	r	w	r	w	r	w	r	w	r	w	r	w	r	w	r
Amur			-1.22	-0.78	0.14	-0.18					0.46	0.11	1.75	0.09			0.51	-1.35	-0.71	-0.10	0.08	-0.46
Copper	0.33	-0.32	-0.35	-0.42	0.59	0.02	-0.47	-0.35	-0.33	0.20	0.14	-0.18	0.89	-0.19	0.32	0.42	0.84	-0.01	0.07	0.03	-1.02	-0.20
Indigirka			-0.35	-0.80	0.03	0.02					1.23	-0.27	0.42	-0.10			0.79	-0.95	-0.02	-0.04	-1.10	-1.15
Mississippi			0.33	-0.14	0.02	-0.45					-0.09	0.39	0.31	0.28			-0.13	-0.06	0.25	0.02	0.30	0.24
Murray-Darling			1.01	0.75	0.08	0.74					-0.12	0.91	0.01	0.93			0.08	0.81	0.34	0.40	-0.41	0.84
Olenek			-0.35	-0.76	0.08	-0.12					2.07	-0.16	-0.95	-0.18			0.28	-0.70	0.10	-0.03	-0.22	-0.83
Parana			0.26	0.01	0.16	-0.19					-0.88	0.34	0.18	0.48			0.20	-0.12	1.29	0.06	-0.21	0.36
Pechora			-0.38	-0.34	0.33	-0.15					0.84	-0.13	0.82	-0.21			-0.01	-0.42	-0.47	-0.01	-0.14	-0.41
Yenisei			-0.71	-0.71	-0.10	-0.21					2.20	-0.09	-0.96	-0.09			0.52	-0.65	0.39	-0.01	-0.33	-0.72

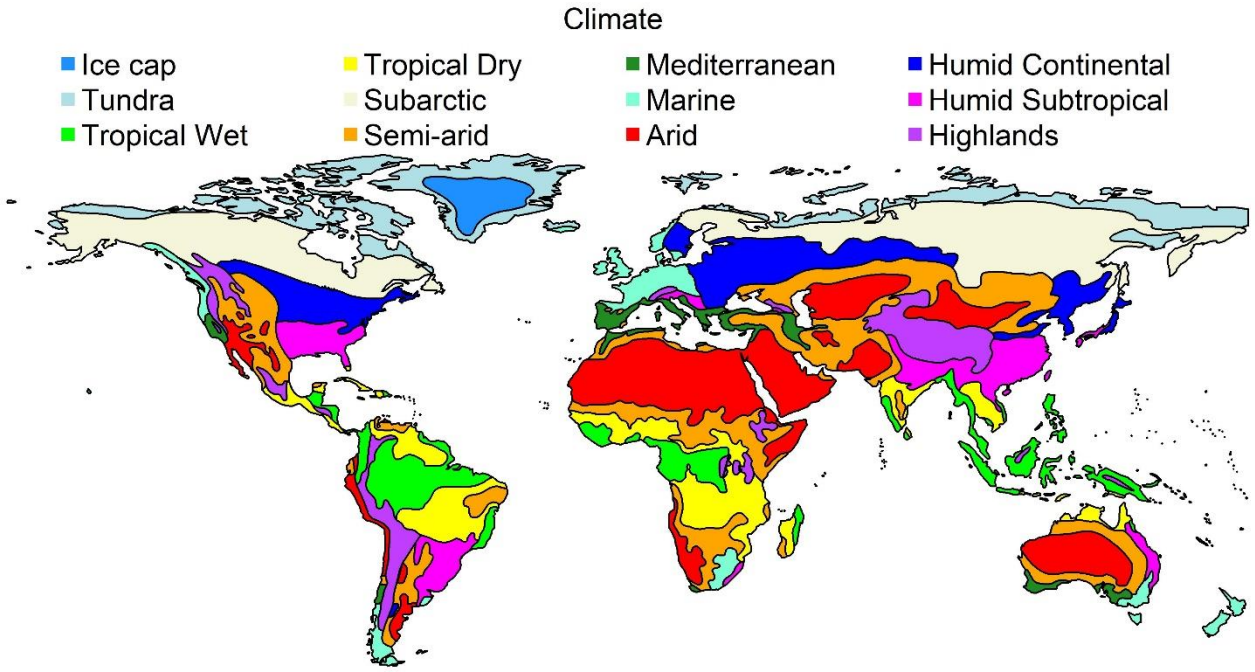

Figure S1: Climate map used in this study (available from ArcGIS online). It is a simplified climate zones map consisting of 12 broad climate classes.

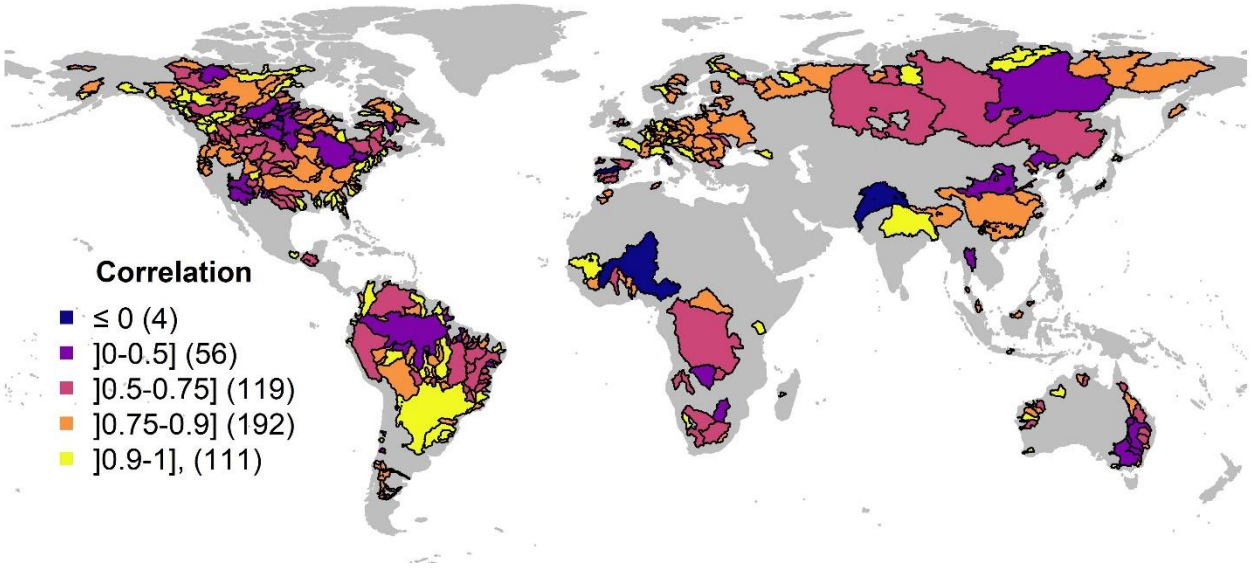

Figure S2: Temporal correlation of LORA with the observed streamflow over the gauged basins. Basins are colour coded by correlation range and their numbers are given in brackets.

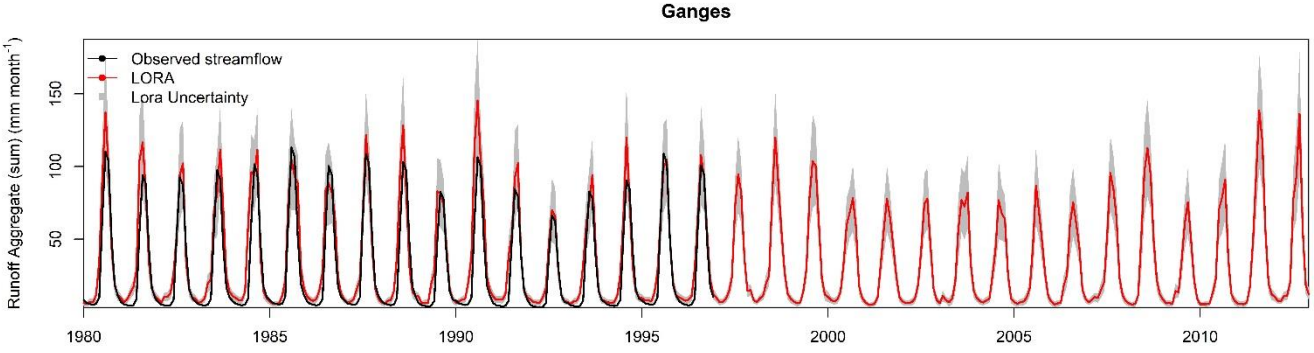

Figure S3: observed streamflow (in black), LORA Runoff aggregate (in red), and its uncertainty range (grey) over the Ganges basin (in mm month^{-1}). This basin was shown in yellow in Fig. S2, indicating that LORA exhibits a high temporal correlation (≥ 0.9) with the observation.

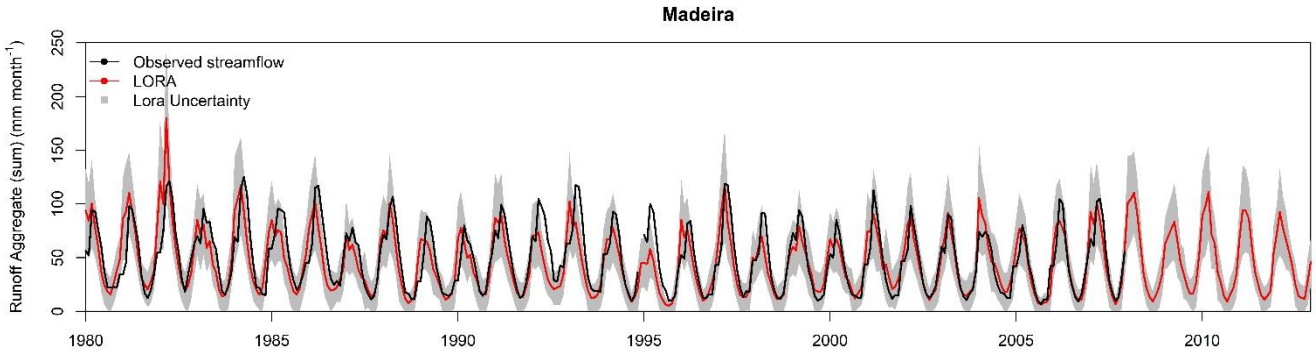

Figure S4: observed streamflow (in black), LORA Runoff aggregate (in red), and its uncertainty range (grey) over Madeira basin, i.e. a sub-basin of the Amazon (in mm month^{-1}). This basin was shown in orange in Fig. S2, indicating that LORA exhibits a temporal correlation in the range [0.75 – 0.9[with the observation.

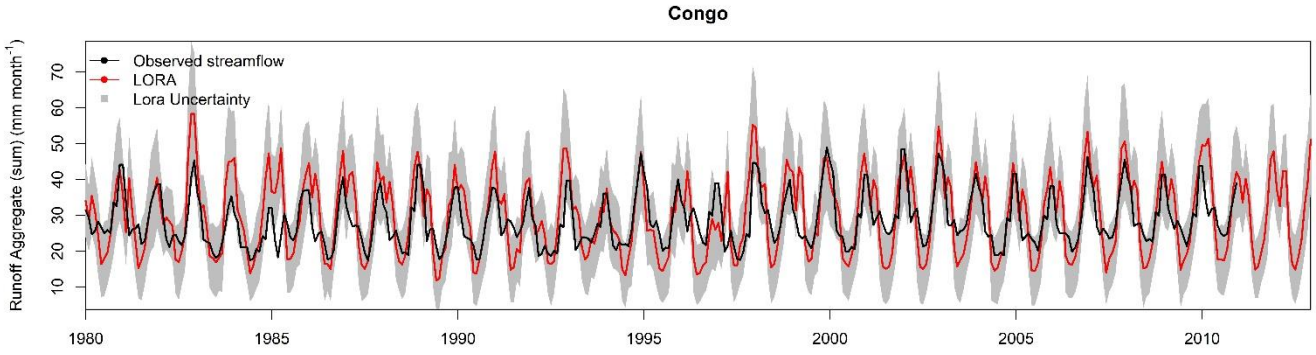

Figure S5: observed streamflow (in black), LORA Runoff aggregate (in red), and its uncertainty range (grey) over the Congo basin (in mm month^{-1}). This basin was shown in violet in Fig. S2, indicating that LORA exhibits a temporal correlation in the range [0.5 – 0.75[with the observation.

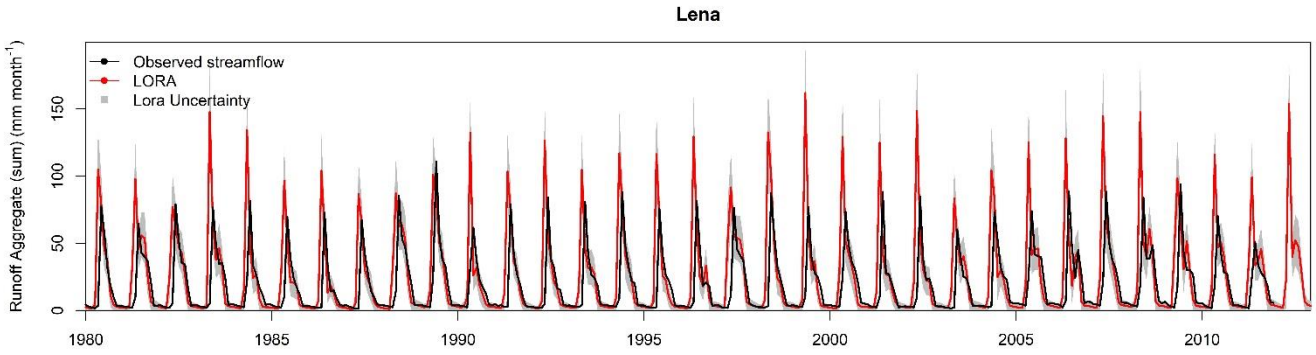

Figure S6: observed streamflow (in black), LORA Runoff aggregate (in red), and its uncertainty range (grey) over Lena basin (in mm month^{-1}). This basin was shown in purple in Fig. S2, indicating that LORA exhibits low temporal correlation (≤0.5) with the observation.

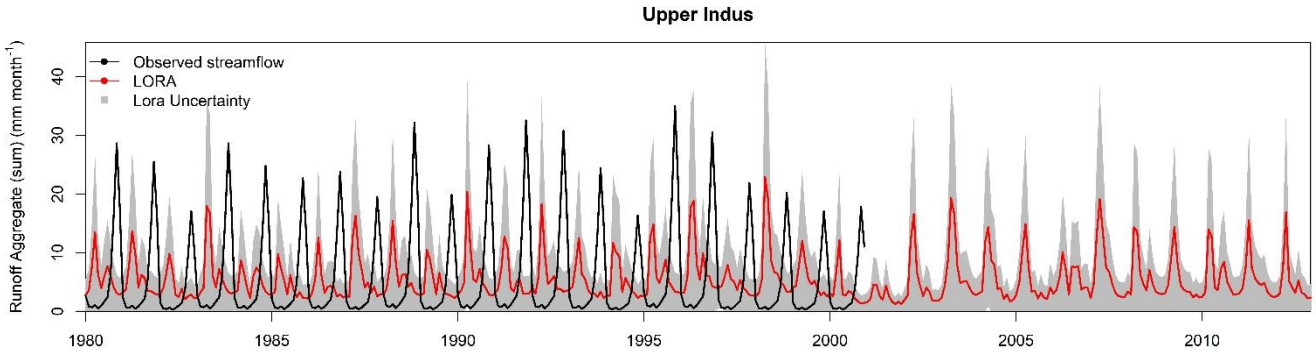

Figure S7: observed streamflow (in black), LORA Runoff aggregate (in red), and its uncertainty range (grey) over the upper Indus basin (in mm month^{-1}). This basin was shown in dark blue in Fig. S2, indicating that LORA exhibits a negative temporal correlation with the observation.

5

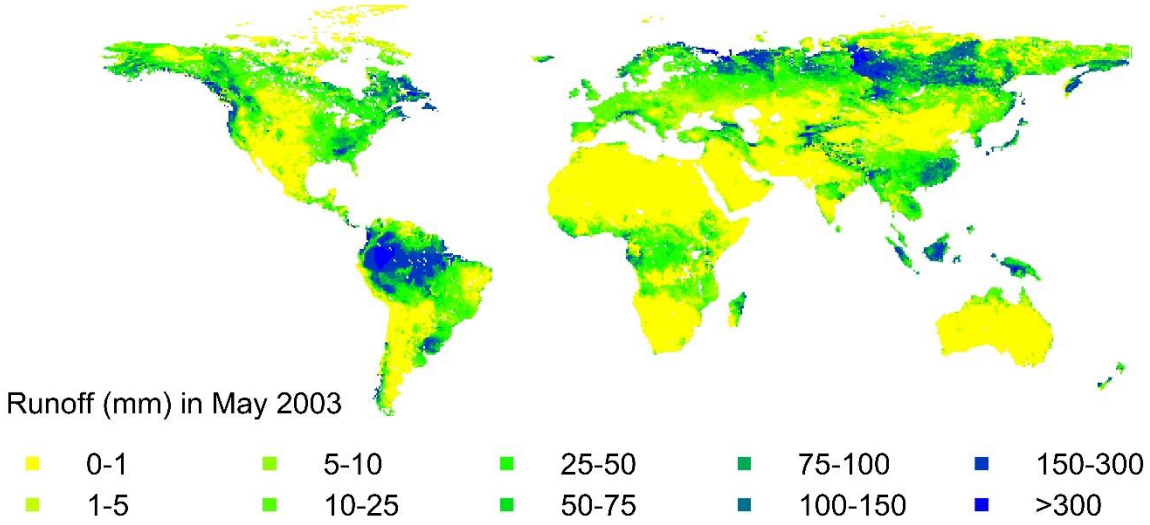

Fig. S8: Global map of LORA runoff fields (mm) in May 2003

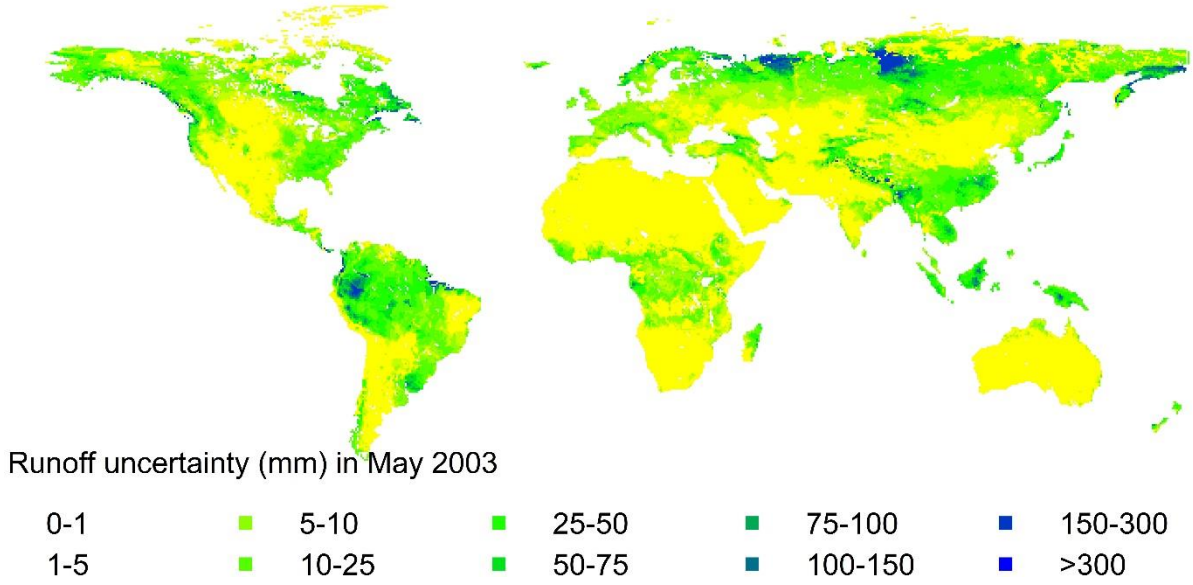

Fig. S8: Global map of LORA uncertainty fields (mm) in May 2003